Time-domain finite-element modeling of three-dimensional seismoelectric waves

Jun Li[1], Changchun Yin[1*], Yang Su[1], Libao Wang[2], Bo Zhang[1], Xiuyan Ren[1], and Yunhe Liu[1]
[1]College of Geoexploration Science and Technology, Jilin University, Changchun, China.
yinchangchun@jlu.edu.cn
[2]Shandong Huichuang Technology Co., Ltd, Shandong, China.

SUMMARY

We propose a three-dimensional time-domain finite-element method for the solution of seismoelectric waves in saturated porous media. Since the electroosmotic feedback is weak, we ignore the mechanical disturbance of the electromagnetic field caused by seismic waves. In this way, we can decouple the electrodynamic coupling equation and solve seismic and electromagnetic waves separately. For the simulation of the seismic waves, we use the explicit finite-element method, where we replace the consistent mass matrix by the lumped mass matrix to make the equation explicitly recursive. Additionally, we leverage the perfectly matched layer to handle the seismic boundary. The seismic wavefield obtained by solving the poroelastic equations is used as the source term to simulate the electromagnetic waves using the finite-element method. Considering the huge velocity difference between electromagnetic and seismic waves, we use an unconditionally stable implicit time recursion when solving the electromagnetic waves. By combining explicit and implicit algorithms, the stability problems with the seismic and electromagnetic modeling can be solved at higher efficiency. By comparing our time-domain finite-element algorithm with the analytical solution for a full-space model, we verified the accuracy of our algorithm.

Keywords: Seismoelectric waves, finite-element, numerical modelling, wave propagation

INTRODUCTION

In saturated fluid media, the electrokinetic effect based on the electric double layer can cause coupling between seismic and electromagnetic (EM) waves (Haartsen and Pride 1997; Zhu et al. 2000). Since the seismic and EM signals generated during the seismoelectric conversion are sensitive to the mechanical and fluid properties of the underground medium, they have great prospects of application in the exploration of oil and gas reservoir (Thompson et al. 2007; Wang et al. 2021).

Since Pride (1994) proposed a set of seismoelectric coupling equations (Pride 1994), scholars have carried out theoretical simulations. These include the analytical methods, e.g. the Green's function and general reflectivity method (Gao and Hu 2010; Ren et al. 2010) as well as the numerical ones such as the finite-difference (FD) and finite-element (FE) methods (Haines and Pride 2006; Li et al. 2023). However, the analytical method cannot handle irregular anomalies. Due to the limitations with the computer memory and calculation speed, three-dimensional (3D) numerical algorithms are facing big challenges. The existing FD and FE methods use two-dimensional (2D) grids for forward modeling of seismoelectric fields. When the model is complex or the underground structure changes significantly in all directions, the 2D forward modeling can no longer effectively simulate the seismoelectric responses of 3D models. In order to better understand the propagation mechanism of seismoelectric effects, we proposed here a 3D time-domain finite-element (FETD) method to solve seismoelectric waves.

In this paper, based on the decoupling strategy, we first use the explicit FE method to solve the displacement field, and then use it as the source to solve the EM fields implicitly. In this way, we can improve the computational efficiency by combining explicit and implicit time recursion. We then test our FETD algorithm by comparing our numerical results with the analytical solution.

METHODS

We simulate the seismoelectric waves based on Pride's seismoelectric coupling equations and consider the wave propagating in 3D space, and assume the *z*-axis positive downward. Since the electroosmotic feedback term is weak that can be ignored (Haines and Pride 2006), the Pride's equations can be simplified to

$$\nabla \cdot \boldsymbol{\tau} + \boldsymbol{F} = \rho \frac{\partial^2 \mathbf{u}}{\partial t^2} + \rho_f \frac{\partial^2 \mathbf{w}}{\partial t^2} \tag{1}$$

$$-\nabla P + \boldsymbol{f} = \rho_f \frac{\partial^2 \mathbf{u}}{\partial t^2} + \frac{\rho_f \alpha_\infty}{\varphi} \frac{\partial^2 \mathbf{w}}{\partial t^2} + \frac{\eta_f}{k} \frac{\partial \mathbf{w}}{\partial t} \tag{2}$$

$$\boldsymbol{\tau} = \left[(H-2G)\nabla\cdot\mathbf{u} + C\nabla\cdot\mathbf{w}\right]\mathbf{I} + G(\nabla\mathbf{u} + \nabla\mathbf{u}^T) \tag{3}$$

$$-P = C\nabla\cdot\mathbf{u} + M\nabla\cdot\mathbf{w} \tag{4}$$

$$\nabla\times\mathbf{H} = \sigma\mathbf{E} + L\frac{\eta_f}{k}\frac{\partial}{\partial t}\mathbf{w} \tag{5}$$

$$\nabla\times\mathbf{E} = -\mu\frac{\partial\mathbf{H}}{\partial t} \tag{6}$$

where **u**, **w** are the solid and relative fluid-solid displacements, **E**, **H** are the EM fields. ***F***, ***f*** are the forces excited on the entire porous medium and fluid, respectively. The meaning of the other parameters can be found from Li et al. (2023).

Note that the poroelastic and EM equations are completely decoupled. This allows us to first solve the poroelastic equations (1)-(4). Here we use the FE method for our solution. The global mass matrix formed after FE discretization is replaced by a lumped mass matrix (Hinton et al. 1976) to simplify the solution process and to improve the calculation efficiency. Using the mass concentration technology we can diagonalize the mass matrix so that the poroelastic equations can be solved based on a simple explicit time recursion scheme (Newmark scheme). It is worth noting that in the computational domain, it is necessary to absorb the outgoing waves to avoid false reflections at the boundary, so we use the complex-frequency-shift unsplit perfect matched layer (CFS-UPML) to absorb seismic waves (Xie et al. 2014).

Furthermore, we use the calculated relative fluid-solid displacement as the source term of Equations (5)-(6) to further solve EM fields. In this paper, we only study the electrostatic near field of EM disturbance, with the influence of induction being ignored. Therefore, Equation (6) can be rewritten as $\nabla\times\mathbf{E} = 0$. Here, we introduce the electric potential, so that $\mathbf{E} = -\nabla\Phi$. Taking the divergence of Equation (5) yields the Poisson equation for the electric potential that is solved by the FE method. To ensure the stability of the numerical solution, the Courant stability condition needs to be applied. Since the velocity of EM waves is much larger than the seismic waves, to improve calculation efficiency, we use unconditionally stable implicit time recursion to solve the Poisson equation. Then, the electric field can be obtained by calculating the negative gradient of the electric potential.

RESULTS

In this section, we simulate the seismoelectric responses for a 3D full-space model. To verify the accuracy of our algorithm, we compared our FETD results with the analytical solutions given by Gao and Hu (2010).

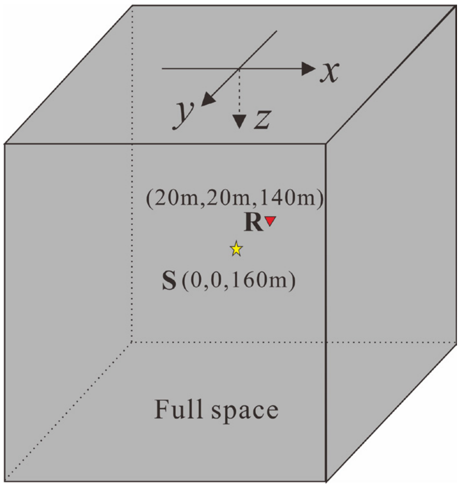

Figure 1. Schematic diagram of the simulation model. The yellow star represents the source and the red triangle represents the receiving point.

Figure 1 shows a schematic diagram of the full-space model of our simulation. The entire model is divided into 180×180×180 grids, with 10 layers of EM grids expanded in each of the three directions, and 10 layers of absorbing layers laid inside the expansion layer. The grid sizes in three directions are all 2 m, and the time step is 0.01 ms. We take an explosion source with M_0 = 1000 N·m for our simulation and assume that the source time function is a 40 Hz Ricker wavelet. The source is located at (0, 0, 160m) and the receiving point is located at (20m, 20m, 140m). The parameters of porous media are listed in Table 1.

Table 1. Parameters of porous medium.

Symbol	Parameters
$\rho_s(\mathrm{kg\cdot m^{-3}})$	2650
$\rho_f(\mathrm{kg\cdot m^{-3}})$	1000
φ	0.2
α_∞	3
$k_s(\mathrm{Gpa})$	12.2
$k_f(\mathrm{Gpa})$	1.985
$k_{fr}(\mathrm{Gpa})$	9.6
$\eta_f(\mathrm{Pa\ s})$	0.001
$G(\mathrm{Gpa})$	5.1
$k(\mathrm{m^2})$	10^{-12}
$v_p(\mathrm{m\cdot s^{-1}})$	2694.7
$v_s(\mathrm{m\cdot s^{-1}})$	1482.7
$L(\mathrm{sC\cdot kg^{-1}})$	20.74×10^{-10}
$\sigma(\mathrm{S\cdot m^{-1}})$	0.00618

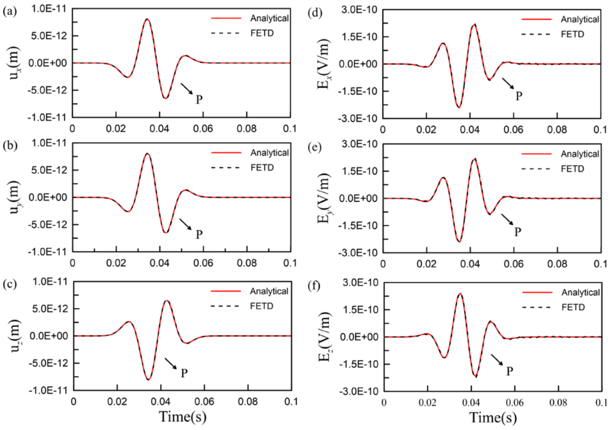

Figure 2. Comparison of our FETD results with analytical solutions for a full-space model excited by an explosion source. (a), (b), and (c) are the x, y, and z component of the solid displacements; while (d), (e), and (f) are the x, y, and z component of the electric fields, respectively.

The solid displacement and electric field calculated by the analytical method (the red solid lines) and our FETD results (the black dashed lines) are shown in Figure 2. The symbol ‘P’ in Figure 2(a)-(c) represents the direct P wave, while the symbol ‘P’ in Figure 2(d)-(f) represents the accompanying electric field generated by the direct P wave. It is seen that our FETD results match well the analytical solutions, which verifies the effectiveness of our algorithm for seismoelectric modelling.

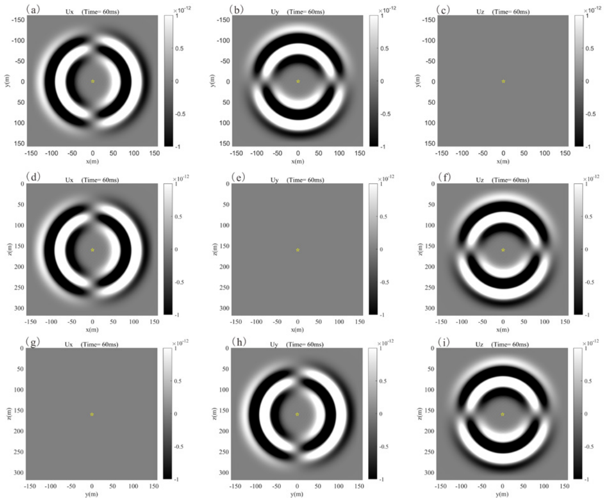

Figure 3. Wavefield snapshot of solid displacement excited by explosion source at t = 60 ms. (a), (b), (c) are the x, y, and z component of the *xy* plane, (d), (e), (f) are the x, y, and z component of the *xz* plane, while (g), (h), (i) are the x, y, and z component of the *yz* plane, respectively.

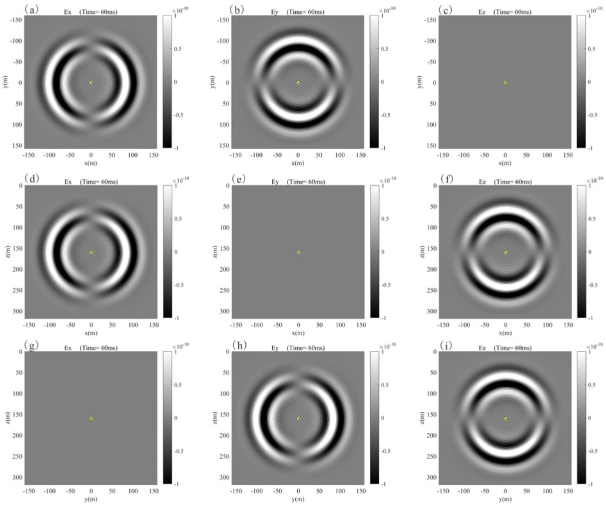

Figure 4. Wavefield snapshot of electric field excited by explosion source at t = 60 ms. (a), (b), (c) are the x, y, and z component of the *xy* plane, (d), (e), (f) are the x, y, and z component of the *xz* plane, while (g), (h), (i) are the x, y, and z component of the *yz* plane, respectively.

Figures 3 and 4 show wavefield snapshots of the solid displacement and electric field at 60 ms, respectively. The figures in each row of Figure 3 and Figure 4 are the x, y, and z components in slice along the three planes (*xy*, *xz*, *yz*) with the source as the center. Taking the *xy* plane as example, the explosion source propagates outward uniformly and generates only P waves. At this time, there exist only *x* and *y* components, the z component is null. From Figures 3 (a) and 3(b), we can see the wavefront of P wave in the snapshots of solid displacement, while in Figures 4(a) and 4(b), we can see the accompanying electric fields of the corresponding P wave. The z component does not appear in the wavefield snapshots of the solid displacement and its accompanying electric field (Figure 3(c) and Figure 4(c)). The same observations can be found in other slices.

CONCLUSIONS

We propose a 3D FETD algorithm to solve the seismoelectric wavefield in porous media. After decoupling Pride’s equations, we can separately solve the seismic and EM waves. Using the explicit FE method to solve the seismic waves and using the implicit FE method for EM equations with the obtained displacement field as the source term, we can efficiently solve for seismic and EM waves. The comparison with the analytical solution for a full-space model has verified the accuracy of our algorithm. More experiments (not presented here for limited space) showed that our algorithm can provide a technical means for numerical simulation of the seismoelectric waves for complex 3D models.

ACKNOWLEDGEMENTS

We want to thank Prof. Yongxin Gao from Hefei University of Technology for his technical support. This study was supported by the National Natural Science Foundation of China (42030806, 42174167, 42274093, 42304149).

REFERENCES

Gao Y, Hu H (2010) Seismoelectromagnetic waves radiated by a double couple source in a saturated porous medium. Geophysical Journal International 181(2), 873-896

Haartsen MW, Pride SR (1997) Electroseismic waves from point sources in layered media. Journal of Geophysical Research: Solid Earth 102(B11), 24745-69

Haines SS, Pride SR (2006). Seismoelectric numerical modeling on a grid. Geophysics 71(6), N57-N65

Hinton E, Rock T, Zienkiewicz OC (1976) A note on mass lumping and related processes in the finite element method. Earthquake Engineering & Structural Dynamics 4(3), 245-249

Li J, Yin C, Liu Y, Wang L, Ma X (2023). Simulation of Seismoelectric Waves Using Time-Domain Finite-Element Method in 2D PSVTM Mode. Remote Sensing 15(13), 3321

Pride S (1994) Governing equations for the coupled electromagnetics and acoustics of porous media. Phys. Rev. B 50(21), 15678-96

Ren H, Huang Q, Chen X (2010) A new numerical technique for simulating the coupled seismic and electromagnetic waves in layered porous media. Earthquake Science 23(2), 167-76

Thompson AH, Hombostel S, Burns J, Murray T, Raschke R, Wridel J, et al. (2007) Field tests of electroseismic hydrocarbon detection. Geophysics 72(1), N1-N9

Wang D, Gao Y, Tong P, Wang J, Yao C, Wang B (2021) Electroseismic and seismoelectric responses at irregular interfaces: possible application to reservoir exploration. Journal of Petroleum Science and Engineering 202, 108513

Xie Z, Komatitsch D, Martin R, Matzen R (2014) Improved forward wave propagation and adjoint-based sensitivity kernel calculations using a numerically stable finite-element PML. Geophysical Journal International 198(3), 1714-1747

Zhu Z, Haartsen MW, Toksöz MN (2000) Experimental studies of seismoelectric conversions in fluid-saturated porous media. Journal of Geophysical Research: Solid Earth 105(B12), 28055-64